# High-spin study of $^{111}$I

E. S. Paul,[1] K. Starosta,[2,*] A. J. Boston,[1] C. J. Chiara,[2] M. Devlin,[3,†] O. Dorvaux,[4,‡] D. B. Fossan,[2] P. T. Greenlees,[4] K. Helariutta,[4] P. Jones,[4] R. Julin,[4] S. Juutinen,[4] H. Kankaanpää,[4] H. Kettunen,[4] D. R. LaFosse,[3,§] G. J. Lane,[2,‖] I. Y. Lee,[5] A. O. Macchiavelli,[5] M. Muikku,[4] P. Nieminen,[4] P. Rahkila,[4] D. G. Sarantites,[3] H. C. Scraggs,[1] J. M. Sears,[2] A. T. Semple,[1] J. F. Smith,[2,¶] and O. Stezowski[1,**]

[1]*Oliver Lodge Laboratory, University of Liverpool, P.O. Box 147, Liverpool L69 7ZE, United Kingdom*

[2]*Department of Physics and Astronomy, State University of New York at Stony Brook, Stony Brook, New York 11794-3800*

[3]*Department of Chemistry, Washington University, St. Louis, Missouri 63130*

[4]*Department of Physics, University of Jyväskylä, P.O. Box 35, FIN-40351, Jyväskylä, Finland*

[5]*Nuclear Science Division, Lawrence Berkeley National Laboratory, Berkeley, California 94720*

(Received 20 January 2000; published 19 May 2000)

A level scheme is presented for $^{111}_{53}$I, populated by the $^{58}$Ni($^{58}$Ni,$\alpha p$) reaction. A backed-target experiment, at a low beam energy of 210 MeV, was performed using the JUROSPHERE spectrometer, while a thin-target experiment at 250 MeV was performed using the GAMMASPHERE spectrometer in conjunction with the MICROBALL charged-particle detector array. The new level scheme fits well the systematics of light iodine nuclei and provides evidence for a terminating band at the highest spins. Low-lying transitions previously assigned to $^{111}$I could not be confirmed.

PACS number(s): 27.60.+j, 23.20.Lv, 21.10.Re

## I. INTRODUCTION

Negative-parity yrast bands built on an $h_{11/2}$ proton intruder orbital have been established in light odd-$A$ iodine isotopes down to $^{113}$I. The $^{109}$I isotope, which lies beyond the proton dripline, has also had corresponding transitions assigned using the technique of recoil-decay tagging (RDT) [1,2]. Two experiments have, however, assigned different $\gamma$ rays to $^{109}$I [2,3]. The $h_{11/2}$ band in the intermediate $^{111}$I isotope is unknown, but an isomeric $I^{\pi}=11/2^{-}$ state has been proposed, together with the decay $\gamma$ rays, following a NORDBALL experiment in conjunction with charged-particle and neutron ancillary detectors [4].

This paper presents a new level scheme for $^{111}$I, deduced from two $^{58}$Ni+$^{58}$Ni experiments, while the previously assigned $\gamma$ rays [4] could not be confirmed. The present experiments were undertaken to investigate the high-spin structure of $^{111}$I, in particular the $\pi h_{11/2}$ band, in order to complete the systematics of the light odd-$A$ iodine isotopes and possibly shed light on the conflicting results for $^{109}$I. Furthermore, the observation of a band to high $\gamma$-ray energies (rotational frequencies) is suggestive of a smoothly terminating configuration in this nucleus.

## II. EXPERIMENTAL DETAILS

### A. Backed-target experiment

Since neutron evaporation from compound systems is severely hindered in this proton-rich mass region, it was decided to populate $^{111}$I using the $^{58}$Ni($^{58}$Ni,$\alpha p$)$^{111}$I fusion-evaporation reaction. A low beam energy (210 MeV) is needed to enhance two-particle evaporation relative to competing $3p$, $4p$, and $\alpha 2p$ channels. Although the total fusion cross section rapidly falls off at such a low beam energy, yield can be recovered by using an intense beam ($10pnA$). A further potential problem may be the low amount of spin brought into the system; classically $l_{\max}\sim 17\hbar$, but states up to $27\hbar$ have already been identified in $^{114}$Xe from the present data [5]. Moreover, recent work on the $^{58}$Ni+$^{60}$Ni system at energies around the classical Coulomb barrier has identified states up to $30\hbar$ in the evaporation residues [6], including the corresponding $\alpha p$ channel into $^{113}$I, implying that the reaction mechanism is more complex than the simple classical picture. The present experiment employed a thin $^{58}$Ni target foil of thickness 600 $\mu$g/cm$^2$ backed by 17 mg/cm$^2$ of $^{197}$Au to maintain pristine energy resolution and a powerful $\gamma$-ray spectrometer was used such that a $\gamma^3$ (triples) coincidence analysis was possible. The excellent energy resolution and triple coincidence analysis were crucial to this study since most of the new transitions assigned to $^{111}$I are degenerate with transitions in other nuclei.

The $^{58}$Ni beam was supplied by the K130 cyclotron at the accelerator laboratory of the University of Jyväskylä (JYFL), Finland. The JUROSPHERE $\gamma$-ray spectrometer, containing seven TESSA-type [7], five NORDBALL-type [8] and fourteen EUROGAM-type [9] HPGe detectors, each within a

*On leave from: Institute of Experimental Physics, Warsaw University, Hoża 69, 00-681 Warsaw, Poland.

†Present address: LANSCE-3, Los Alamos National Laboratory, Los Alamos, New Mexico 87545.

‡Present address: Institut de Recherches Subatomiques, F-67037-Strasbourg Cedex 2, France.

§Present address: Department of Physics and Astronomy, State University of New York at Stony Brook, Stony Brook, New York 11794.

‖Present address: Nuclear Science Division, Lawrence Berkeley National Laboratory, Berkeley, California 94720.

¶Present address: Schuster Laboratory, University of Manchester, Brunswick Street, Manchester M13 9PL, United Kingdom.

**Present address: IPN Lyon, IN2P3-CNRS, Université C. Bernard Lyon-1, F-69622 Villeurbanne Cedex, France.

 

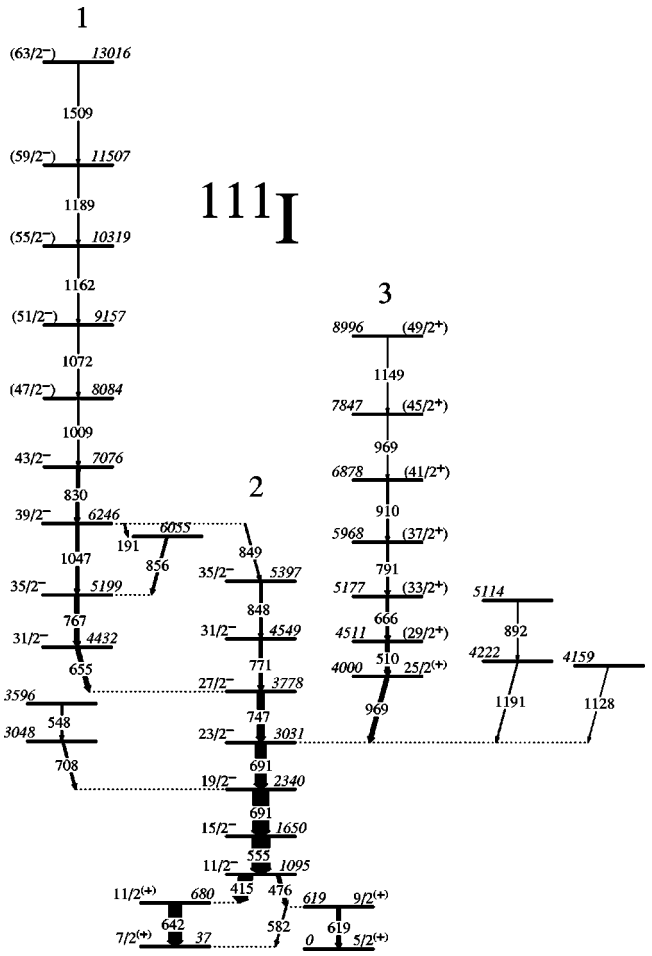


FIG. 1. Level scheme deduced for $^{111}$I from this work. The transition energies are given in keV and their relative intensities are proportional to the widths of the arrows. Absolute spin and parity assignments are taken from systematics, starting with the $11/2^-$ bandhead of band 2.

bismuth-germanate escape-suppression shield, was used to record $\gamma$-ray coincidences of fold two and above. Approximately $3.6\times10^8$ events were recorded, of which 80% were $\gamma-\gamma$ and 16% $\gamma-\gamma-\gamma$ coincidences. A 2D matrix and a 3D cube were built from the data and analyzed using the RADWARE graphical analysis package [10].

### B. Thin-target experiment

This experiment was carried out at the 88-Inch Cyclotron of the Lawrence Berkeley National Laboratory, prior to the JUROSPHERE experiment. High-spin states in $A\sim110$ nuclei were populated with the $^{58}$Ni($^{58}$Ni,$x\alpha ypzn\gamma$) fusion-evaporation reaction at 250 MeV. The beam was incident on two thin self-supporting nickel targets, each of nominal thickness 500 $\mu$g/cm$^2$. The higher beam energy was used to preferentially populate three- and four-particle exit channels; this experiment was not designed for two-particle exit channels such as $^{111}$I ($\alpha p$). Nevertheless, the combination of the GAMMASPHERE [11] $\gamma$-ray spectrometer with the MICROBALL [12] charged-particle detector allowed selection of the $\alpha p$ channel. For this experiment, GAMMASPHERE contained only 83 escape-suppressed HPGe detectors since the forward 15 detectors were replaced with neutron detectors.

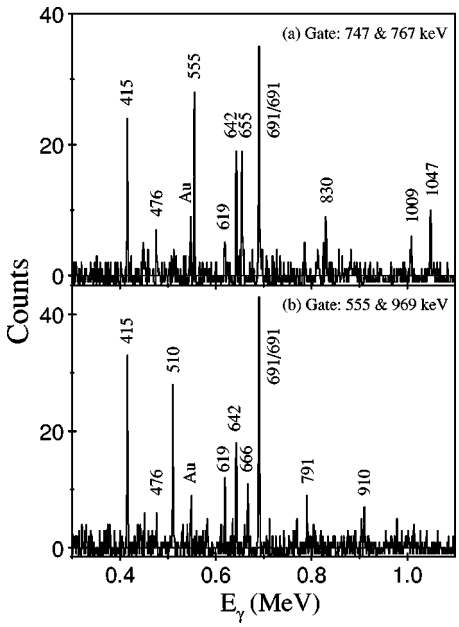


FIG. 2. Examples of gated coincidence spectra, obtained from the backed-target data, with transition energies labeled in keV: (a) Spectrum double gated by the 747- and 767-keV transitions of band 1. (b) Spectrum double gated by the 555- and 969-keV transitions. Contaminant transitions from the Coulomb excitation of the gold backing are labeled by ''Au.''

A kinematic Doppler reconstruction [12,13], performed using the MICROBALL, yielded an improvement of 30% in the energy resolution of $\gamma$-ray transitions. This was especially important given the high recoil velocity of this symmetric reaction with $v/c\approx4.5\%$. In order to further improve channel selection, the BGO anti-Compton shield elements of GAMMASPHERE were used as a $\gamma$-ray fold and sum-energy selection device; to achieve this the Hevimet collimators were removed from the front of the HPGe detectors, allowing $\gamma$ rays to directly strike the shield elements. The number of BGO elements firing and their total summed energy were recorded for each event providing fold ($k$) and sum-energy ($H$) information. By setting off-line software gates on a two dimensional $k$-$H$ plot, a significant improvement in the quality of the channel selection was made. Specifically, high $k$ and $H$ values enhanced the two-particle $^{111}$I channel.

A total of $1.4\times10^9$ events were recorded. Gamma rays selected for $^{111}$I ($\alpha p$ and high $k$-$H$) were replayed into RADWARE format [10,14] matrices ($\gamma^2$), cubes ($\gamma^3$), and hypercubes ($\gamma^4$) for subsequent level scheme construction.

## III. RESULTS

The new level scheme deduced for $^{111}$I is shown in Fig. 1, where the ordering of transitions is based on relative $\gamma$-ray intensities and coincidence relationships. Examples of double-gated $\gamma$-ray coincidence spectra, extracted from the backed-target data, are presented in Fig. 2. Measured transi-

TABLE I. Measured properties of the $\gamma$-ray transitions assigned to $^{111}$I from the backed-target experiment. Absolute spin and parity assignments are taken from systematics.

| $E_\gamma$ (keV)[a] | Relative intensity[b] | Angular intensity ratio $R$[c] | Multipolarity | Assignment |
|---|---|---|---|---|
| 191.4 | 1 | | | $39/2^- \rightarrow$ |
| 415.0 | 76 | 0.97(5) | $E1$ $(\Delta I=0)$ | $11/2^- \rightarrow 11/2^{(+)}$ |
| 475.9 | 19 | 0.66(5) | $E1$ | $11/2^- \rightarrow 9/2^{(+)}$ |
| 510.3 | 18 | | | $(29/2^+) \rightarrow 25/2^{(+)}$ |
| 555.1 | $\equiv 100$ | 0.97(3)[d] | $E2$ | $15/2^- \rightarrow 11/2^-$ |
| 581.7 | 5 | 0.72(9) | $M1/E2$ | $9/2^{(+)} \rightarrow 7/2^{(+)}$ |
| 618.9 | 14 | 0.98(7)[d] | $E2$ | $9/2^{(+)} \rightarrow 5/2^{(+)}$ |
| 642.5 | 71 | 1.02(4) | $E2$ | $11/2^{(+)} \rightarrow 7/2^{(+)}$ |
| 654.6 | 34 | 1.06(8) | $E2$ | $31/2^- \rightarrow 27/2^-$ |
| 666.5 | 13 | 1.06(9) | $E2$ | $(33/2^+ \rightarrow 29/2^+)$ |
| 690.6 | 140[e] | 1.01(3)[e] | $E2$ | $19/2^- \rightarrow 15/2^-$ |
| 690.6 | 140[e] | 1.01(3)[e] | $E2$ | $23/2^- \rightarrow 19/2^-$ |
| 708.4 | 3 | | | $\rightarrow 19/2^-$ |
| 747.2 | 26 | 0.96(8)[d] | $E2$ | $27/2^- \rightarrow 23/2^-$ |
| 766.7 | 22 | 1.07(9) | $E2$ | $35/2^- \rightarrow 31/2^-$ |
| 770.8 | 16 | 1.11(10) | $E2$ | $31/2^- \rightarrow 27/2^-$ |
| 790.8 | 11 | 1.03(10) | $E2$ | $(37/2^+ \rightarrow 33/2^+)$ |
| 829.7 | 9 | 1.11(13) | $E2$ | $43/2^- \rightarrow 39/2^-$ |
| 848.4 | 9[e] | 0.97(12)[e] | $E2$ | $35/2^- \rightarrow 31/2^-$ |
| 848.4 | 9[e] | 0.97(12)[e] | $E2$ | $39/2^- \rightarrow 35/2^-$ |
| 856.2 | 1 | | | $\rightarrow 35/2^-$ |
| 909.9 | 6 | 0.98(14) | $E2$ | $(41/2^+ \rightarrow 37/2^+)$ |
| 969.5 | 20 | 0.60(6) | $E1$ | $25/2^{(+)} \rightarrow 23/2^-$ |
| 1008.5 | 5 | | | $(47/2^-) \rightarrow 43/2^-$ |
| 1047.4 | 12 | 1.12(11) | $E2$ | $39/2^- \rightarrow 35/2^-$ |

[a] $\gamma$-ray energies are accurate to $\pm 0.2$ keV.
[b] Errors on the relative intensities are estimated to be less than 5% of the quoted values.
[c] Except where stated, the $R$ values were obtained from spectra gated by the 555 keV transition.
[d] $R$ value obtained using the 691-keV transitions as the gate.
[e] Value given for composite peak.

tion energies and the relative intensities of the $^{111}$I $\gamma$ rays from this data set are listed in Table I.

Relative spins and parities were inferred through an angular-correlation analysis [15] of the backed-target data set, as described in Ref. [5]. Gamma rays recorded in the ''central'' JUROSPHERE detectors, near $\theta = 90°$, were sorted against those recorded in the ''backward'' detectors into an asymmetric $\gamma\gamma$ matrix. Gamma-ray intensities were extracted from gated spectra projected onto the central and backward axes of this matrix, respectively, and an average angular-intensity ratio, defined as

$$R = \frac{I_\gamma(\text{measured backward, gated central})}{I_\gamma(\text{measured central, gated backward})}, \qquad (1)$$

was evaluated for the transitions of $^{111}$I. Transitions of stretched-quadrupole character $(\Delta I = 2)$ were identified by $R$ values of approximately 1.00 when gated by a stretched $E2$ transition, although pure nonstretched dipole $(\Delta I = 0)$ transitions are also expected to possess similar ratios. Values of $R \approx 0.65$ are expected for transitions of pure stretched-dipole character $(\Delta I = 1)$. The results of this analysis for the $^{111}$I transitions are included in Table I.

Absolute spin/parity assignments are made from systematics. In particular, an $I^\pi = 11/2^-$ bandhead is expected for the $\pi h_{11/2}$ band, while a $5/2^+$ ground state ($\pi d_{5/2}$) is expected together with a low-lying $7/2^+$ state ($\pi g_{7/2}$). The 476-keV transition depopulating the $11/2^-$ state of band 2,

TABLE II. Measured yields of various nuclei for the $^{58}$Ni + $^{58}$Ni reaction at 210 MeV compared to predicted cross sections (ALICE).

| Nucleus | Channel | Yield (%)[a] | ALICE $\sigma$ (mb) |
|---|---|---|---|
| $^{113}$I | $3p$ | 100 | 97 |
| $^{114}$Xe | $2p$ | 35 | 50 |
| $^{112}$Te | $4p$ | 30 | 25 |
| $^{110}$Te | $\alpha 2p$ | 26 | 26 |
| $^{113}$Xe | $2pn$ | 5.2 | 5.2 |
| $^{111}$I | $\alpha p$ | 4.5 | 7.0 |

[a] Errors are estimated to be less than 5% of the quoted values.

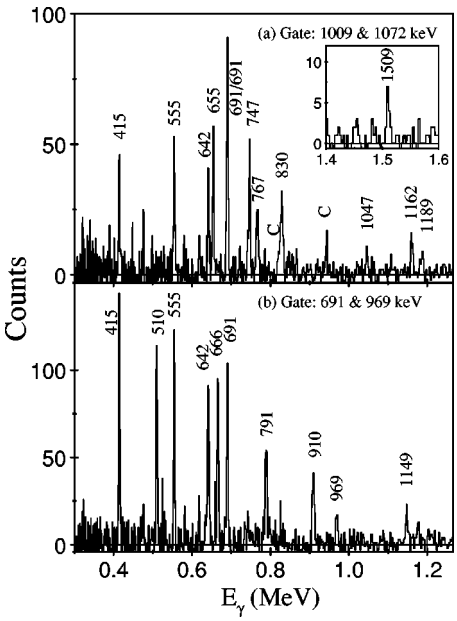


FIG. 3. Examples of gated coincidence spectra, obtained from the thin-target data, with transition energies labeled in keV: (a) Spectrum double gated by the 1009- and 1072-keV transitions of band 1. The inset shows the topmost 1509-keV transition. Peaks labeled ''C'' are contaminants. (b) Spectrum double gated by the 691 and 969 keV transitions. Note that 691- and 969-keV transitions appear in this spectrum, showing that they are both self-coincident doublets.

together with the 969-keV transition feeding the $23/2^-$ state of band 2, have angular-intensity ratios consistent with stretched-dipole transitions and an $E1$ multipolarity is proposed. This suggests that the low-lying levels are of positive parity, as expected from systematics, together with band 3. An exact energy doublet is placed connecting $23/2^- - 19/2^- - 15/2^-$ levels; the adjacent placement of the two 691-keV transitions is corroborated by triple coincidence relationships with the transitions of bands 1 and 3.

Table II shows measured yields of nuclei produced in the backed-target data, together with predictions from the ALICE fusion-evaporation code [16]. It should be noted that, apart from $^{111}$I, all the nuclei in Table II have been well studied with large $\gamma$-ray spectrometers. Furthermore, the new transitions shown in Fig. 1 are not in coincidence with transitions of these other nuclei, implying they form a separate level scheme in a different nucleus. The measured yield is similar to that predicted for the $\alpha p$ channel and hence the new transitions are assigned to $^{111}$I. The distribution of exit channels in Table II is also very similar to that measured for the $^{58}$Ni+$^{60}$Ni reaction at a similar beam energy [6]. Indeed, in this case $^{113}$I, the corresponding $\alpha p$ channel, was observed at a similar population intensity. Apart from the nuclei listed in Table II, no other known nuclei could be identified. Moreover, the previously assigned transitions of $^{111}$I [4] could not be confirmed in the present work. The previous assignment was made, however, using a reaction at a very high energy ($^{58}$Ni+$^{54}$Fe at 270 MeV). Although a thick target (10 mg/cm$^2$) was used such that energies down to the Coulomb barrier were achieved within it, the desired $1p$ evaporation channel would be overwhelmed by competing multiparticle channels.

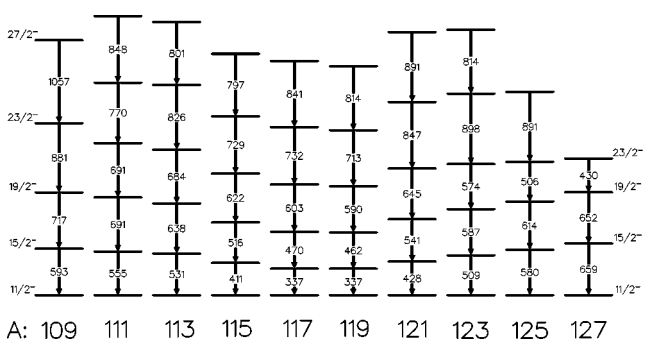


FIG. 4. Systematics of odd-$A$ iodine isotopes. The $^{109}$I results are taken from Ref. [3].

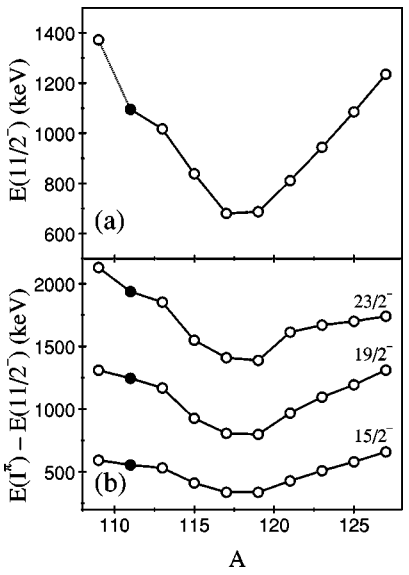


FIG. 5. Systematics of $11/2^-$ bandhead energies (a) and energies of negative-parity states relative to the $11/2^-$ state (b) in odd-$A$ iodine isotopes. The solid symbols correspond to the new $^{111}$I levels. The excitation energy of the $11/2^-$ state in $^{109}$I in (a) is tentative [3].

With the new level scheme proposed for $^{111}$I, a search was made of the thin-target data set in order to confirm the assignment. The new transitions are indeed enhanced in the $\alpha p$-gated data, thus corroborating the assignment of the transitions to $^{111}$I. Double-gated spectra observed from this data set are shown in Fig. 3. The thin-target data extended band 1 to higher spin with the observation of high-energy ($>1$ MeV) transitions. Band 3 was also extended with the observation of a doublet of energy 969 keV. Again, the transitions previously assigned to $^{111}$I [4] were not seen.

## IV. DISCUSSION

The systematics of $\pi h_{11/2}$ bands in the light iodine isotopes are shown in Fig. 4. The new $11/2^-$, $15/2^-$, and $19/2^-$ states of $^{111}$I fit well between those of the neighboring isotopes, taking the transitions of Ref. [3] for $^{109}$I. The energies

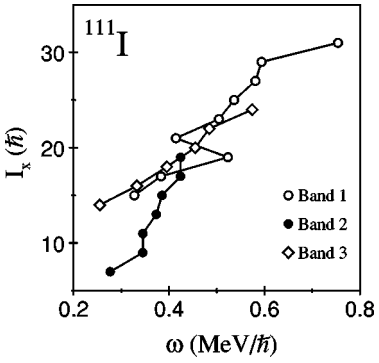


FIG. 6. Aligned angular momentum, $I_x$, of the bands in $^{111}$I plotted as a function of rotational frequency.

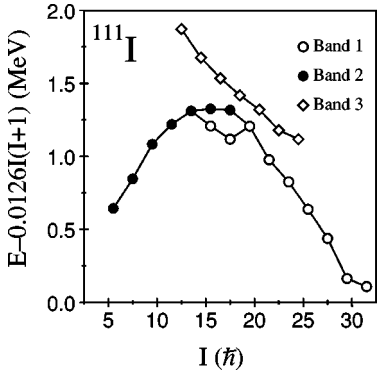


FIG. 7. Energies of the levels in $^{111}$I, minus a rigid-rotor reference, plotted as a function of spin.

of these low-lying levels in the odd-$A$ iodine isotopes are also plotted in Fig. 5 together with the excitation energy of the $11/2^-$ bandhead. It appears that the level spacings for the lightest two iodine isotopes ($^{109,111}$I) do not rise as quickly as those for the heavier isotopes on the opposite side of the semimagic neutron number 64 ($^{117}$I). The excitation energy of the present $h_{11/2}$ bandhead in $^{111}$I is also lower than expected (n.b. that of $^{109}$I is tentative). These observations imply that the deformation is changing more slowly than expected for the lightest isotopes. Maximum deformation occurs for $^{117,119}$I ($N=64,66$) and decreases on both sides of these isotopes. A similar situation occurs for the lightest Xe isotopes [17] where the deformation also appears to decrease more slowly than expected. Following a systematic comparison of the energy levels of the nuclei in this mass region, it has been proposed that the underlying cores for $\nu h_{11/2}$ bands in odd-$A$ Te isotopes are more deformed than corresponding even-even neighbors [18], while the cores for the $\pi h_{11/2}$ bands in the lightest iodine isotopes seem to be stiffer [19], i.e., less susceptible to polarization effects of the valence particle in a high-$j$ proton orbital.

The total aligned angular momentum, $I_x=\sqrt{I(I+1)-K^2}$, of the bands in $^{111}$I are plotted as a function of rotational frequency in Fig. 6. The behavior is rather irregular, suggesting that $^{111}$I is not a perfect rotor. The energies of the levels in $^{111}$I, minus a rigid-rotor reference, are plotted as a function of spin in Fig. 7; again, the behavior is somewhat irregular. Deformation self-consistent cranking calculations based on the total-Routhian surface (TRS) formalism [20–22], employing a triaxial Woods-Saxon single-particle potential [23,24], indicate a $\gamma$-soft shape with quadrupole deformation $\beta_2\approx 0.16$–$0.18$. Band 1 probably involves a pair of rotationally aligned $\nu h_{11/2}$ quasineutrons coupled to the odd $\pi h_{11/2}$ quasiproton. Candidate structures for band 3 are $\pi d_{5/2}\otimes[\nu(h_{11/2})^2]$ or $\pi h_{11/2}\otimes[\nu h_{11/2}g_{7/2}]$ configurations with signature $\alpha=+1/2$ (favored component).

Calculations for $^{111}$I based on the cranked Nilsson-Strutinsky approach had predicted that smoothly terminating configurations are near the yrast line [25,26]. Above spin $I=30\hbar$ these configurations involve promoting particles from $\pi g_{9/2}$ orbitals, originating below the $Z=50$ shell gap, into $\pi h_{11/2}$ intruder orbitals. Below this spin, however, configurations with no $\pi g_{9/2}$ holes, which terminate at spins just above $30\hbar$, are favored [26]. In the formalism of Ref. [26], a negative-parity configuration of the type $[p_1p_2,n]=[01,2]$ is expected, where $p_1$ represents the number of $\pi g_{9/2}$ holes, $p_2$ represents the number of $\pi h_{11/2}$ particles, and $n$ represents the number of $\nu h_{11/2}$ particles, respectively. Only the occupation of these orbitals, relative to the $^{100}$Sn core, is labeled; the remaining valence particles are distributed over $g_{7/2}$ and $d_{5/2}$ orbitals from the N=4 oscillator shell. The [01,2] configuration could correspond to band 1 and is consistent with the quasiparticle configuration proposed earlier. The [01,2] configuration terminates at $I^\pi=67/2^-$, which is only $2\hbar$ more than the topmost level of band 1. Furthermore, the termination is predicted to be relatively flat in a rigid-rotor plot, rather than show the usual upturn which is associated with a high energy cost to form the final states of the band [26]. This is consistent with the experimental rigid-rotor plot for band 1 shown in Fig. 7.

## V. CONCLUSIONS

A new level scheme has been deduced for $^{111}$I, while the previously assigned transitions [4] could not be confirmed. The new low-lying levels fit the systematics of neighboring nuclei well, especially the levels of $^{109}$I proposed by Ref. [3] rather than those of Ref. [2]. The level scheme has been observed up to a proposed spin and parity $63/2^-$. The high-spin behavior is suggestive of a terminating band which is predicted to terminate just $2\hbar$ higher than seen here.

## ACKNOWLEDGMENTS

The JUROSPHERE project is supported in part by grants from the U.K. EPSRC and the French IN2P3. Support for this work was also provided by the Academy of Finland and the Large Scale Facility program under the TMR program of the European Union. This work was also supported in part by the U.S. National Science Foundation. The authors are indebted to Dr. D. C. Radford for providing the RADWARE analysis codes.

[1] R. S. Simon, K.-H. Schmidt, F. P. Hessberger, S. Hlavac, M. Honusek, G. Munzenberg, H.-G. Clerc, U. Gollerthan, and W. Schwab, Z. Phys. A **325**, 197 (1986).
[2] E. S. Paul, P. J. Woods, T. Davinson, R. D. Page, P. J. Sellin, C. W. Beausang, R. M. Clark, R. A. Cunningham, S. A. Forbes, D. B. Fossan, A. Gizon, J. Gizon, K. Hauschild, I. M. Hibbert, A. N. James, D. R. LaFosse, I. Lazarus, H. Schnare, J. Simpson, R. Wadsworth, and M. P. Waring, Phys. Rev. C **51**, 78 (1995).
[3] C.-H. Yu, A. Galindo-Uribarri, S. D. Paul, M. P. Carpenter, C. N. Davids, R. V. F. Janssens, C. J. Lister, D. Seweryniak, J. Uusitalo, and B. D. MacDonald, Phys. Rev. C **59**, R1834 (1999).
[4] M. Karny, J. Kownacki, D. Seweryniak, A. Atac, B. Cederwall, C. Fahlander, A. Johnson, A. Kerek, L.-O. Norlin, J. Nyberg, E. Adamides, E. Ideguchi, R. Julin, S. Juutinen, W. Karczmarczyk, S. Mitarai, M. Piiparinen, R. Schubart, G. Sletten, S. Törmänen, and A. Virtanen, Z. Phys. A **350**, 179 (1994).
[5] E. S. Paul, H. C. Scraggs, A. J. Boston, O. Dorvaux, P. T. Greenlees, K. Helariutta, P. Jones, R. Julin, S. Juutinen, H. Kankaanpää, H. Kettunen, M. Muikku, P. Nieminen, P. Rahkila, and O. Stezowski, Nucl. Phys. **A673**, 31 (2000).
[6] S. Courtin, F. Hoellinger, N. Rowley, A. Lopez-Martens, F. Hannachi, O. Stezowski, A. J. Boston, P. Dagnall, J. Durell, C. Finck, B. J.-P. Gall, B. Haas, F. Haas, J. Lisle, A. Lunt, J.-C. Merdinger, E. S. Paul, H. C. Scraggs, B. Varley, and J.-P. Vivien, Acta Phys. Pol. B **30**, 1549 (1999).
[7] P. J. Nolan, D. W. Gifford, and P. J. Twin, Nucl. Instrum. Methods Phys. Res. A **236**, 95 (1985).
[8] B. Herskind, Nucl. Phys. **A447**, 395 (1985).
[9] C. W. Beausang, S. A. Forbes, P. Fallon, P. J. Nolan, P. J. Twin, J. N. Mo, J. C. Lisle, M. A. Bentley, J. Simpson, F. A. Beck, D. Curien, G. DeFrance, G. Duchêne, and D. Popescu, Nucl. Instrum. Methods Phys. Res. A **313**, 37 (1992).
[10] D. C. Radford, Nucl. Instrum. Methods Phys. Res. A **361**, 297 (1995); **361**, 306 (1995).
[11] I. Y. Lee, Nucl. Phys. **A520**, 641c (1990).
[12] D. G. Sarantites, P.-F. Hua, M. Devlin, L. G. Sobotka, J. Elson, J. T. Hood, D. R. LaFosse, J. E. Sarantites, and M. R. Maier, Nucl. Instrum. Methods Phys. Res. A **381**, 418 (1996).
[13] D. Seweryniak, J. Nyberg, C. Fahlander, and A. Johnson, Nucl. Instrum. Methods Phys. Res. A **340**, 353 (1994).
[14] D. C. Radford, M. Cromaz, and C. J. Beyer, in *Proceedings of the Nuclear Structure '98 Conference, Gatlinburg, 1998*, edited by C. Baktash, AIP Conf. Proc. No. 481 (AIP, New York, 1999), p. 570.
[15] K. S. Krane, R. M. Steffen, and R. M. Wheeler, Nucl. Data Tables **11**, 351 (1973).
[16] F. Plasil and M. Blann, Phys. Rev. C **11**, 508 (1975).
[17] J. F. Smith, C. J. Chiara, D. B. Fossan, G. J. Lane, J. M. Sears, M. Devlin, D. R. LaFosse, D. G. Sarantites, A. J. Boston, E. S. Paul, A. T. Semple, I. Y. Lee, and A. O. Macchiavelli, Contribution to the Nuclear Structure '98 meeting, Gatlinburg, 1998, p. 125.
[18] K. Starosta, C. J. Chiara, D. B. Fossan, T. Koike, D. R. LaFosse, G. J. Lane, J. M. Sears, J. F. Smith, A. J. Boston, P. J. Nolan, E. S. Paul, A. T. Semple, M. Devlin, D. G. Sarantites, I. Y. Lee, and A. O. Macchiavelli, Phys. Rev. C **61**, 034308 (1999).
[19] K. Starosta, D. R. LaFosse, C. J. Chiara, D. B. Fossan, T. Koike, G. J. Lane, J. M. Sears, J. F. Smith, A. J. Boston, P. J. Nolan, E. S. Paul, A. T. Semple, M. Devlin, D. G. Sarantites, I. Y. Lee, and A. O. Macchiavelli (unpublished).
[20] W. Nazarewicz, G. A. Leander, and J. Dudek, Nucl. Phys. **A467**, 437 (1987).
[21] R. Wyss, J. Nyberg, A. Johnson, R. Bengtsson, and W. Nazarewicz, Phys. Lett. B **215**, 211 (1988).
[22] W. Nazarewicz, R. Wyss, and A. Johnson, Nucl. Phys. **A503**, 285 (1989).
[23] W. Nazarewicz, J. Dudek, R. Bengtsson, T. Bengtsson, and I. Ragnarsson, Nucl. Phys. **A435**, 397 (1985).
[24] S. Cwiok, J. Dudek, W. Nazarewicz, W. Skalski, and T. Werner, Comput. Phys. Commun. **46**, 379 (1987).
[25] A. V. Afanasjev and I. Ragnarsson, Nucl. Phys. **A591**, 387 (1995).
[26] A. V. Afanasjev, D. B. Fossan, G. J. Lane, and I. Ragnarsson, Phys. Rep. **322**, 1 (1999).